Undocumented potential for primary productivity in a globally-distributed bacterial photoautotroph

Authors: E.D. Graham[1], J.F. Heidelberg[1,2], B.J. Tully[*1,2]

Author Affiliations:

[1]Department of Biological Sciences, University of Southern California, Los Angeles, CA, USA

[2]Center for Dark Energy Biosphere Investigations, University of Southern California, Los Angeles, CA, USA

*Corresponding Author: Benjamin Tully, tully.bj@gmail.com

Keywords: autotrophy; marine carbon cycle; metagenomics; Alphaproteobacteria; aerobic anoxygenic phototrophs

Abstract: Aerobic anoxygenic phototrophs (AAnPs) are common in the global oceans and are associated with photoheterotrophic activity. To date, AAnPs have not been identified in the surface ocean that possess the potential for carbon fixation. Using the *Tara Oceans* metagenomic dataset, we have reconstructed high-quality genomes of four bacteria that possess the genomic potential for anoxygenic phototrophy, carbon fixation via the Calvin-Benson-Bassham cycle, and the oxidation of sulfite and thiosulfate. Forming a monophyletic clade within the *Alphaproteobacteria* and lacking cultured representatives, the organisms compose minor constituents of local microbial communities (0.1-1.0%), but are globally distributed, present in multiple samples from the North Pacific, Mediterranean Sea, the East Africa Coastal Province, and the South Atlantic. These organisms represent a shift in our understanding of microbially-mediated photoautotrophy in the global oceans and provide a previously undiscovered route of primary productivity.

Significance Statement: In examining the genomic content of organisms collected during the *Tara Oceans* expedition, we have identified a novel clade within the *Alphaproteobacteria* that has the potential for photoautotrophy. Based on genome observations, these organisms have the potential to couple inorganic sulfur compounds as electron donors to fix carbon into biomass. They are globally distributed, present in samples from the North Pacific, Mediterranean Sea, East Africa Coastal Current, and the South Atlantic. This discovery may require re-examination of the microbial communities in the global ocean to understand and constrain the impacts of this group of organisms on the global carbon cycle.

Introduction

It has been understood for decades that the basis of the global marine carbon cycle are oxygenic photoautotrophs that perform photoautotrophic processes. Two additional phototrophic processes are common in the ocean and are mediated by proteorhodopsin-containing microorganisms and aerobic anoxygenic phototrophs (AAnPs). Proteorhodopsins and AAnPs have historically been associated with photoheterotrophy[1,2], a process that supplements additional energy to microorganisms beyond what is obtained as part of a heterotrophic metabolic strategy. AAnPs utilize bacteriochlorophyll (BChl *a*), are globally distributed[3], and have been identified in phylogenetically diverse groups of microorganisms[4-6]. Though anaerobic microorganisms with BChl *a* are known to fix CO_2[7] and marine AAnPs can incorporate inorganic carbon via anaplerotic reactions[8], marine AAnPs have not been linked to carbon fixation[9]. The identification of marine AAnPs capable of carbon fixation adds to our understanding of microbial photosynthesis in the global oceans and represents a previously undiscovered route of photoautotrophy.

The *Tara Oceans* expedition generated microbial metagenomes during a circumnavigation of the global oceans[10,11]. *Tara Oceans* samples were collected from 63 sites in 10 major ocean provinces, with most sites contributing multiple sampling depths (generally, surface, deep chlorophyll maximum [DCM], and mesopelagic) and multiple size fractions (generally, 'viral', 'girus' [giant virus], 'bacterial', and 'protistan') from each depth (Supplementary Information 1). We independently assembled each sample and assemblies from all samples within a province were combined and subjected to binning techniques to reconstruct microbial genomes (Fig. 1 and Extended Data Fig. 1). Microbial genomes reconstructed from eight of ten provinces (Mediterranean, Red Sea, Arabian Sea, Indian Monsoon Gyre, East Africa Coastal, South Atlantic, and North Pacific; 36 sites, 134 samples) were annotated using the KEGG Ontology (KO) system[12] and examined for the genes and pathways of interest.

Results and Discussion

From 1,774 metagenome-assembled genomes (MAGs), 53 genomes possessed the genes encoding the core subunits of type-II photochemical reaction centers (PufLM). Of those 53, four genomes (MED800, EAC638, SAT68, NP970; Fig. 1) also contained genes for ribulose-1,5-bisphosphate carboxylase (Rubisco; RbsLS; Fig. 2). Rubisco has four major forms, of which three (Types I, II, and III) have been shown to fix CO_2 and two are known to participate in the Calvin-Benson-Bassham (CBB) cycle (Types I and II[13,14]. Phylogenetic placement of the Rubisco large subunits recovered from the genomes revealed them to be of the Type IC/D subgroup[13], suggesting that the identified proteins represent *bona fide* Rubiscos capable of carbon fixation (Fig. 2). Within the Type IC/D subgroup, the Rubisco sequences from the four analyzed genomes formed a distinct cluster with environmental sequences derived from the Global Ocean Survey (GOS) metagenomes[15,16], but lacking sequences from reference organisms.

Similarly, the PufM sequences from the analyzed *Tara* genomes did not cluster with reference sequences, instead grouping with sequences from the GOS metagenomes[15]. Sequences from MED800, SAT68, and NP970 were group together in one cluster, while EAC638 was located in a separate cluster (Fig. 3). The MED800/SAT68/NP970 clade is basal to the previously identified phylogroups E and F, while the EAC638 clade is basal to the *Roseobacter*-related phylogroup G[17]. As MED800, EAC638, SAT68, and NP970 branch in distinct clades on both the RbsL and PufM trees that consist of entirely environmental sequences, it may be

possible that these clades represent a phylogenetically coherent group of organisms with the potential for both phototrophy and carbon fixation.

The genomes were of high-quality (66-85% complete; <5.5% duplication; Table 1) with sufficient phylogenetic markers for accurate placement (Extended Data Table 1). The four organisms form a monophyletic clade basal to the Family *Rhodobacteraceae* (Fig. 4). The relationship between the genomes would suggest that NP970, SAT68, and MED800 are phylogenetically more closely related to each other than either are to EAC638. As is common with assembled metagenomic sequences, the recovered genomes lack a distinguishable 16S rRNA gene sequence. However, based on the observed phylogenetic distance in the concatenated marker tree, we suggest that these organisms represent a new clade within the *Rhodobacteraceae*, and possibly a family-level clade previously without a reference sequence within the *Alphaproteobacteria*. We propose that NP970, SAT68, and MED800 represent three species within the same genus (tentatively named, '*Candidatus Luxescamonas taraoceani'*), with EAC638 as a representative of a species in a sister genus (tentatively named, '*Candidatus Luxescabacter africus'*).

In addition to Rubisco, all four genomes contained genes encoding phosphoribulokinase, an essential gene of the CBB cycle, and 50-89% of the genes necessary to perform complete carbon fixation (Fig. 5). The BChl *a* genes in MED800, EAC638, SAT68, and NP970 were accompanied by bacteriochlorophyll biosynthesis and light-harvesting genes (Supplementary Information 2). This complement of bacteriochlorophyll biosynthesis and essential carbon fixation genes support a role for autotrophy within these organisms beyond the identified marker genes.

All four genomes possessed ATP-binding cassette (ABC) type transporters for spermidine/putrescine and L- and branched-chain amino acids. These transporters are indicative of the utilization of organic nitrogen compounds, as spermidine and putrescine are nitrogen rich organic compounds, while the scavenging of amino acids reduces the overall nitrogen demands of the cell. Further, the genomes lacked transporters and degradation enzymes for many of the saccharides common in the marine environment[18] (Fig. 5). However, MED800, SAT68, and NP970 possessed an ABC-type α-glucoside transporter, an annotated β-glucosidase in SAT68, and D-xylose and D-ribose ABC-type transporters in EAC638. While autotrophs are generally considered to not require external sources of organic carbon, saccharide transporters are commonly observed in classical photoautotrophic organisms[19,20], including the specific example of α-glucoside transporters in strains of *Synechocystis*[21]. For the four genomes, the minimal number of carbon transport and degradation genes may suggest that the organisms have a limited capacity to utilize dissolved organic carbon compounds, but are capable of heterotrophic growth under certain conditions. As such, the genomic potential of these organisms suggest that NP970, SAT68, MED800, and EAC638 are likely facultative autotrophs or mixotrophs.

In oxygenic photosynthesis, electrons are donated as a result of the oxidation of water. Lacking photosystem II, BChl *a*-containing organisms are incapable of oxidizing water and would require an alternative electron donor for autotrophic processes. EAC638 and SAT68 contained the full/partial suite of genes necessary for thiosulfate oxidation, while MED800, NP970, and SAT68 possessed the genes for oxidizing sulfite. The oxidation of sulfur compounds has previously been linked to autotrophy in the marine environment[22]. The oxidation of organic sulfur compounds, like dimethyl sulfide, has been shown to be a source of thiosulfate[23] and sulfite[24] in the marine environment. Electrons derived from inorganic sulfur sources (thiosulfate

and/or sulfite) could be transferred directly through cytochromes or membrane-bound quinone dehydrogenases to the electron transport chain. Electrons could be shuttled to reaction centers to generate proton motive force necessary to convert NADH to NADPH via transhydrogenase (reverse electron flow) and generate ATP for the CBB cycle (Fig. 5).

The reconstruction of four genomes from the same novel family in four different provinces (North Pacific, Mediterranean, East Africa coastal current, and South Atlantic) suggests that the observed genomes represent an *in situ* microbial population from the surface marine environment. Each of the genomes recruit metagenomic reads from multiple sampling sites in each province and are present at >0.1% of the microbial relative abundance (range: 0.1-1.04%; mean: 0.286%) in 20 samples (Fig. 1; Supplemental Information 1). Predominantly, the genomes were present in samples are located in the surface (n = 5) or DCM (n = 12). These organisms were collected at depths where light was available for photosynthesis and less frequently identified at deeper depths (n = 3 mesopelagic samples). When >0.1% relative abundance, the genomes tend to be more abundant in the 'bacterial'/'girus' size fraction (n = 14), though were also observed in 'protistan' (n = 4), and 'viral' (n = 2) size fractions (Supplemental Information 1). The nature of the 'bacterial' size fractions suggests that these organisms are generally not particle attached and <1.6μm in size. The occurrence in the protistan fraction may be due to slightly larger cells or attachment to particles, but this data are difficult to interpret as the 'protistan' and 'bacterial' size fractions can overlap (0.8-1.6μm). As members of the free-living bacterioplankton, these organisms should be poised to grow in aerobic conditions. All four genomes possessed the genes encoding for cytochromes involved in aerobic metabolisms (aa_3- and bc_1-type), and lacked the genes for cytochromes involved in microaerobic metabolisms and alternative electron acceptors. Further, all four genomes encoded the gene for an oxygen-dependent ring cyclase (*acsF*), a necessary component in bacteriochlorophyll biosynthesis for which there is alternative that is oxygen-independent (*bchE*) and used by anaerobic organisms.

With this discovery, the potential photosynthesis in the ocean has expanded beyond organisms harboring chlorophyll *a* to include *Alphaproteobacteria* with BChl *a*. Though these organisms have not been cultivated or sequenced before, both PufM and Rubisco in MED800, EAC638, NP970, and SAT68 are phylogenetically related to GOS-derived proteins, lending credence to the fact that these organisms may be a persistent element of oceanic carbon fixation. As such, clades of environmentally sampled genes (*rbsL* and *pufM*) can now be linked to a previously unrecognized source of marine primary productivity. Because carbon fixation estimates are broadly estimated by the concentration of chlorophyll compounds (specifically chlorophyll *a*), current values are likely incomplete and do account for the contributions of bacteriochlorophyll-containing, carbon fixing AAnPs. The identification of a globally distributed clade of AAnPs in the ocean capable of carbon fixation continues to expand our understanding of the marine carbon cycle.

Materials and Methods:

Assembly

All sequences for the reverse and forward reads from each sampled station and depth within the *Tara Oceans* dataset were accessed from European Molecular Biology Laboratory (EMBL)[10,11]. Typically, *Tara* sampling sites have multiple metagenomic samples, representing different sampling depths and size fractions. The common size fractions were used during sampling were: 'bacterial' (0.22-1.6μm) (includes Mediterranean 'girus' samples), 'protistan' (0.8-5.0μm),

'girus' (0.45-0.8μm) and 'viral' (<0.22μm). Surface samples were collected at ~5-m depth, while deep chlorophyll maximum (DCM) and mesopelagic depths were variable depending the physiochemical features of the site. Paired-end reads from different filter sizes from each site and depth (e.g., TARA0007, girus filter fraction, sampled at the DCM) were assembled using Megahit[25] (v1.0.3; parameters: --preset, meta-sensitive) (Supplementary Information 1). All of the Megahit assemblies from each province were pooled in to two tranches based on assembly size, <2kb and ≥2kb. Longer assemblies (≥2kb) with ≥99% semi-global identity were combined using CD-HIT-EST[26] (v4.6; -T 90 -M 500000 -c 0.99 -n 10). The reduced set of contiguous DNA fragments (contigs) ≥2kb was then cross-assembled using Minimus2[27] (AMOS v3.1.0; parameters: -D OVERLAP=100 MINID=95).

Binning

Contigs from each province were initially clustered into tentative genomic bins using BinSanity[28]. Due to computational limitations, the South Atlantic, East African Coastal province, and Mediterranean Sea were initially run with contig size cutoffs of 11.5kbp, 7.5kbp, and 7kbp, respectively. The BinSanity workflow was run iteratively three times using variable preference values (v.0.2.5.5; parameters: -p [(1) -10, (2) -5, (3) -3] -m 4000 -v 400 -d 0.95). Between each of the three main clustering steps, refinement was performed based on sequence composition (parameters: -p [(1) -25, (2) -10, (3) -3] -m 4000 -v 400 -d 0.95 -kmer 4). After refinement and before the next pass with BinSanity, bins were evaluated using CheckM[29] (v.1.0.3; parameters: lineage_wf, default settings) for completion and redundancy. High-quality genomes were considered those that were >90% complete with <10% contamination, >80% complete with <5% contamination, or >50% complete with <2% contamination. Bins representing high-quality genomes were removed from subsequent rounds of clustering. After identification of the four genomes of interest (initially 51-84% complete, <7.0% contamination), binning was performed with CONCOCT[30] (v.0.4.1; parameters: -c 800 -I 500) on contigs >5kb from each province that had a produced a genome of interest. To improve completion estimates, overlapping CONCOCT and BinSanity bins were visualized using Anvi'o[31] (v.2.1.0) and manually refined to improve genome completion and minimize contamination estimates (Extended Data Fig. 3-6).

Annotation

Putative DNA coding sequences (CDSs) were predicted for each genome using Prodigal[32] (v.2.6.2; -m -p meta). Putative CDS were submitted for annotation by the KEGG database using BlastKOALA[12] (taxonomy group, Prokaryotes; database, genus_prokaryotes + family_eukaryotes; Accessed March 2017) (Supplementary Information Table 3). Assessment of pathways and metabolisms of interest were determined using the script KEGG-decoder.py (www.github.com/bjtully/BioData/tree/master/KEGGDecoder). Genomes of interested were determined based on the presence of genes assigned as the M subunit of type-II photochemical reaction center (PufLM) and ribulose-1,5-bisphosphate carboxylase (RbsLS). After confirmation of the genes of interest (see below), additional annotations were performed for the genomes using the Rapid Annotation using Subsystem Technology (RAST) service (Classic RAST default parameters - Release70)[33].

Phylogeny

An initial assessment of phylogeny was conducted using pplacer[34] within CheckM. The Prodigal-derived CDSs were searched for a collection of single-copy marker genes that was common to all four *Tara* assembled genomes using hidden Markov models collected from the

Pfam database[35] (Accessed March 2017) and HMMER [36] (v3.1b2; parameters: hmmsearch -E 1e-10 --notextw). 17 marker genes were identified that met this criteria[37-39] (Extended Data Table 1). The 17 markers were identified in 2,889 reference genes from complete and partial genomes accessed from NCBI Genbank[40] (Supplementary Information 4). If a genome contained multiple copies of a single marker gene both were excluded from the final tree. Only genomes containing ≥10 markers were used for phylogenetic placement. Each marker set was aligned using MUSCLE[41] (v3.8.31; parameter: -maxiters 8) and trimmed using TrimAL[42] (v.1.2rev59; parameter: -automated1). Alignments were then manually assessed and concatenated in Geneious[43]. An approximate maximum likelihood tree was generated using FastTree[44] (v.2.1.3; parameters: -gtr -gamma; Supplementary Information 5). A simplified version of this phylogenetic tree was constructed using the same protocol, but with 160 reference genomes for Fig. 2 (Supplementary Information 6 and 7).

Phylogenetic tree – Rubisco and Bacteriochlorophyll

RbsL and PufM sequences representing previously described lineages were collected[13,17] (Supplementary Information 8 and 9). Additional reference PufM sequences were collected from environmentally generated bacterial artificial chromosomes[5] and Integrated Microbial Genomes (IMG; Accessed Feb 2017)[45]. Protein sequences from IMG were assessed based on genomes with KEGG Ontology (KO) annotations[46] for the reaction center subunit M (K08929). PufM sequences from Prodigal predicted CDS (as above) of Global Ocean Survey (GOS) assemblies[16] were identified using DIAMOND[47] (v.0.8.36.98; parameters: BLASTP, default settings), where all reference and *Tara* genome sequences were used as a query. Two separate phylogenetic trees were constructed (RbsL and PufM) using the following methodology. Sequences were aligned using MUSCLE[41] (parameter: -maxiters 8) and automatically trimmed using TrimAL[42] (parameter: -automated1) (Supplementary Information 10 and 11). After manual assessment, trimmed alignments were used to construct approximately-maximum-likelihood phylogenetic trees using FastTree[44] (parameters: -gtr -gamma) (Supplementary Information 12 and 13).

Relative abundance of genomes in each sample

Reads from each sample were recruited against all assemblies ≥2kb from the same province using Bowtie2[48] (parameters: default settings), under the assumptions that contigs <2kb would include, low abundance bacteria and archaea, bacteria and archaea with high degrees of repeats/assembly poor regions, fragmented picoeukaryotic genomes, and problematic read sequences (low quality, sequencing artefacts, etc.). For the four sets of contigs (North Pacific, Mediterranean, East Africa Coastal province, and South Atlantic), putative CDS were determined via Prodigal (parameters: see above). In order to estimate the relative abundance of the four analyzed genomes within the bacteria and archaea portion of the total microbial community (excluding eukaryotes and viruses), single-copy marker genes were identified using a collection of previously identified HMMs[49,50] and searched using HMMER[36] (hmmsearch --notextw --cut_tc). Markers belonging to the four genomes were isolated from the total set of environmental markers. The number of reads aligned to each marker was determined using BEDTools[51] (v2.17.0; multicov default parameters). Length-normalized relative abundance values were determined for each genome (Supplementary Information 1):

$$\frac{\sum \text{Reads bp}^{-1} \text{ genome markers}}{\sum \text{Reads bp}^{-1} \text{ metagenome contig markers}} \times 100$$

Data availability

Data is available… submission to NCBI is ongoing. [Currently data is available at FigShare, including high resolution copies of figures, contig and protein sequences, and all supplementary information files: **https://figshare.com/s/9f603e9bbef71164e61b**]

References:

1. Béjá, O., Spudich, E. N., Spudich, J. L., Leclerc, M. & DeLong, E. F. Proteorhodopsin phototrophy in the ocean. *Nature* **411,** 786–789 (2001).
2. Harashima, K., Kawazoe, K., Yoshida, I. & Kamata, H. Light-Stimultated Aerobic Growth of Erythrobacter Species Och-114. *Plant and Cell Physiology* **28,** 365–374 (1987).
3. Schwalbach, M. S. & Fuhrman, J. A. Wide-ranging abundances of aerobic anoxygenic phototrophic bacteria in the world ocean revealed by epifluorescence microscopy and quantitative PCR. *Limnology and Oceanography* **50,** 620–628 (2005).
4. Koblížek, M. Ecology of aerobic anoxygenic phototrophs in aquatic environments. *FEMS Microbiol. Rev.* **39,** 854–870 (2015).
5. Béjá, O. *et al.* Unsuspected diversity among marine aerobic anoxygenic phototrophs. *Nature* **415,** 630–633 (2002).
6. Kang, I. *et al.* Genome Sequence of Fulvimarina pelagi HTCC2506T, a Mn(II)-Oxidizing Alphaproteobacterium Possessing an Aerobic Anoxygenic Photosynthetic Gene Cluster and Xanthorhodopsin. *J. Bacteriol.* **192,** 4798–4799 (2010).
7. Frigaard, N.-U. Biotechnology of Anoxygenic Phototrophic Bacteria. *Adv. Biochem. Eng. Biotechnol.* **156,** 139–154 (2016).
8. Hauruseu, D. & Koblížek, M. Influence of Light on Carbon Utilization in Aerobic Anoxygenic Phototrophs. *Appl. Environ. Microbiol.* **78,** 7414–7419 (2012).
9. Moran, M. A. *et al.* Deciphering ocean carbon in a changing world. *Proceedings of the National Academy of Sciences* **113,** 3143–3151 (2016).
10. Pesant, S. *et al.* Open science resources for the discovery and analysis of Tara Oceans data. *Sci. Data* **2,** 150023–16 (2015).
11. Sunagawa, S. *et al.* Ocean plankton. Structure and function of the global ocean microbiome. *Science* **348,** 1261359–1261359 (2015).
12. Kanehisa, M., Sato, Y. & Morishima, K. BlastKOALA and GhostKOALA: KEGG Tools for Functional Characterization of Genome and Metagenome Sequences. *Journal of Molecular Biology* **428,** 726–731 (2016).
13. Tabita, F. R. *et al.* Function, Structure, and Evolution of the RubisCO-Like Proteins and Their RubisCO Homologs. *Microbiol. Mol. Biol. Rev.* **71,** 576–599 (2007).
14. Badger, M. R. & Bek, E. J. Multiple Rubisco forms in proteobacteria: their functional significance in relation to CO2 acquisition by the CBB cycle. *Journal of Experimental Botany* **59,** 1525–1541 (2007).
15. Rusch, D. B. *et al.* The Sorcerer II Global Ocean Sampling Expedition: Northwest Atlantic through Eastern Tropical Pacific. *Plos Biol* **5,** e77 (2007).
16. Venter, J. C. *et al.* Environmental genome shotgun sequencing of the Sargasso Sea. *Science* **304,** 66–74 (2004).
17. Yutin, N. *et al.* Assessing diversity and biogeography of aerobic anoxygenic phototrophic bacteria in surface waters of the Atlantic and Pacific Oceans using the Global Ocean Sampling expedition metagenomes. *Environ. Microbiol.* **9,** 1464–1475 (2007).
18. Baker, B. J., Lazar, C. S., Teske, A. P. & Dick, G. J. Genomic resolution of linkages in carbon, nitrogen, and sulfur cycling among widespread estuary sediment bacteria. *Microbiome* **3,** 14 (2015).
19. Gómez-Baena, G. *et al.* Glucose Uptake and Its Effect on Gene Expression in Prochlorococcus. *PLoS ONE* **3,** e3416–11 (2008).
20. Michelou, V. K., Cottrell, M. T. & Kirchman, D. L. Light-Stimulated Bacterial Production and Amino Acid Assimilation by Cyanobacteria and Other Microbes in the North Atlantic Ocean. *Appl. Environ. Microbiol.* **73,** 5539–5546 (2007).
21. Kaneko, T. *et al.* Sequence analysis of the genome of the unicellular cyanobacterium Synechocystis sp. strain PCC6803. II. Sequence determination of the entire genome and assignment of potential protein-coding regions. *DNA Res.* **3,** 109–136 (1996).

22. Swan, B. K. *et al.* Potential for Chemolithoautotrophy Among Ubiquitous Bacteria Lineages in the Dark Ocean. *Science* **333,** 1296–1300 (2011).
23. de Zwart, J., Nelisse, P. N. & Kuenen, J. G. Isolation and characterization of Methylophaga sulfidovorans sp nov: An obligately methylotrophic, aerobic, dimethylsulfide oxidizing bacterium from a microbial mat. *FEMS Microbiol. Ecol.* **20,** 261–270 (1996).
24. Kelly, D. P., Baker, S. C., Trickett, J., Davey, M. & Murrell, J. C. Methanesulphonate utilization by a novel methylotrophic bacterium involves an unusual monooxygenase. *Microbiology* **140,** 1419–1426 (1994).
25. Li, D. *et al.* MEGAHIT v1.0: A fast and scalable metagenome assembler driven by advanced methodologies and community practices. *Methods* **102,** 3–11 (2016).
26. Fu, L., Niu, B., Zhu, Z., Wu, S. & Li, W. CD-HIT: accelerated for clustering the next-generation sequencing data. *Bioinformatics* **28,** 3150–3152 (2012).
27. Treangen, T. J., Sommer, D. D., Angly, F. E., Koren, S. & Pop, M. Next generation sequence assembly with AMOS. *Curr Protoc Bioinformatics* **Chapter 11,** Unit 11.8 (2011).
28. Graham, E. D., Heidelberg, J. F. & Tully, B. J. BinSanity: unsupervised clustering of environmental microbial assemblies using coverage and affinity propagation. *PeerJ* **5,** e3035–19 (2017).
29. Parks, D. H., Imelfort, M., Skennerton, C. T., Hugenholtz, P. & Tyson, G. W. CheckM: assessing the quality of microbial genomes recovered from isolates, single cells, and metagenomes. *Genome Res.* **25,** 1043–1055 (2015).
30. Alneberg, J. *et al.* Binning metagenomic contigs by coverage and composition. *Nat Meth* **11,** 1144–1146 (2014).
31. Eren, A. M. *et al.* Anvi'o: an advanced analysis and visualization platform for 'omics data. *PeerJ* **3,** e1319 (2015).
32. Hyatt, D., LoCascio, P. F., Hauser, L. J. & Uberbacher, E. C. Gene and translation initiation site prediction in metagenomic sequences. *Bioinformatics* **28,** 2223–2230 (2012).
33. Aziz, R. K. *et al.* The RAST Server: Rapid Annotations using Subsystems Technology. *BMC Genomics* **9,** 75 (2008).
34. Matsen, F. A., Kodner, R. B. & Armbrust, E. V. pplacer: linear time maximum-likelihood and Bayesian phylogenetic placement of sequences onto a fixed reference tree. *BMC Bioinformatics* **11,** 538 (2010).
35. Bateman, A. *et al.* The Pfam Protein Families Database. *Nucleic Acids Res.* **30,** 276–280 (2002).
36. Finn, R. D., Clements, J. & Eddy, S. R. HMMER web server: interactive sequence similarity searching. *Nucleic Acids Res.* **39,** W29–W37 (2011).
37. Wu, D., Jospin, G. & Eisen, J. A. Systematic Identification of Gene Families for Use as 'Markers' for Phylogenetic and Phylogeny-Driven Ecological Studies of Bacteria and Archaea and Their Major Subgroups. *PLoS ONE* **8,** e77033–11 (2013).
38. Santos, S. R. & Ochman, H. Identification and phylogenetic sorting of bacterial lineages with universally conserved genes and proteins. *Environ. Microbiol.* **6,** 754–759 (2004).
39. Alexandre, A., Laranjo, M., Young, J. P. W. & Oliveira, S. dnaJ is a useful phylogenetic marker for alphaproteobacteria. *Int. J. Syst. Evol. Microbiol.* **58,** 2839–2849 (2008).
40. Benson, D. A. *et al.* GenBank. *Nucleic Acids Res.* **28,** 15–18 (2000).
41. Edgar, R. C. MUSCLE: multiple sequence alignment with high accuracy and high throughput. *Nucleic Acids Res.* **32,** 1792–1797 (2004).
42. Capella-Gutiérrez, S., Silla-Martínez, J. M. & Gabaldón, T. trimAl: a tool for automated alignment trimming in large-scale phylogenetic analyses. *Bioinformatics* **25,** 1972–1973 (2009).
43. Kearse, M. *et al.* Geneious Basic: an integrated and extendable desktop software platform for the organization and analysis of sequence data. *Bioinformatics* **28,** 1647–1649 (2012).
44. Price, M. N., Dehal, P. S. & Arkin, A. P. FastTree 2--approximately maximum-likelihood trees for large alignments. *PLoS ONE* **5,** e9490 (2010).
45. Markowitz, V. M. *et al.* The integrated microbial genomes (IMG) system. *Nucleic Acids Res.* **34,** D344–8 (2006).
46. Kanehisa, M., Sato, Y., Kawashima, M., Furumichi, M. & Tanabe, M. KEGG as a reference resource for gene and protein annotation. *Nucleic Acids Res.* **44,** D457–D462 (2016).
47. Buchfink, B., Xie, C. & Huson, D. H. Fast and sensitive protein alignment using DIAMOND. *Nat Meth* **12,** 59–60 (2014).
48. Langmead, B. & Salzberg, S. L. Fast gapped-read alignment with Bowtie 2. *Nat Meth* **9,** 357–359 (2012).
49. Albertsen, M. *et al.* Genome sequences of rare, uncultured bacteria obtained by differential coverage binning of multiple metagenomes. *Nat Biotechnol* **31,** 533–538 (2013).

50. Tully, B. J. & Heidelberg, J. F. Potential Mechanisms for Microbial Energy Acquisition in Oxic Deep-Sea Sediments. *Appl. Environ. Microbiol.* **82,** 4232–4243 (2016).
51. Quinlan, A. R. & Hall, I. M. BEDTools: a flexible suite of utilities for comparing genomic features. *Bioinformatics* **26,** 841–842 (2010).

Acknowledgments:

We would like to acknowledge and thank Drs. Eric Webb and William Nelson for providing invaluable comments and critiques in the early stages of this research. We are indebted to the *Tara Oceans* consortium for their commitment to open-access data that allows data aficionados to indulge in the data and attempt to add to the body of science contained within. And we thank the Center for Dark Energy Biosphere Investigations (C-DEBI) for providing funding to BJT and JFH (OCE-0939654). This is C-DEBI contribution number ###.

Author contributions: BJT conceived of the research plan, performed analysis, and wrote the manuscript. EDG performed analysis and wrote the manuscript. JFH provided funding, provided guidance, and edited the manuscript.

Competing financial interests: The authors declare no conflict of interest.

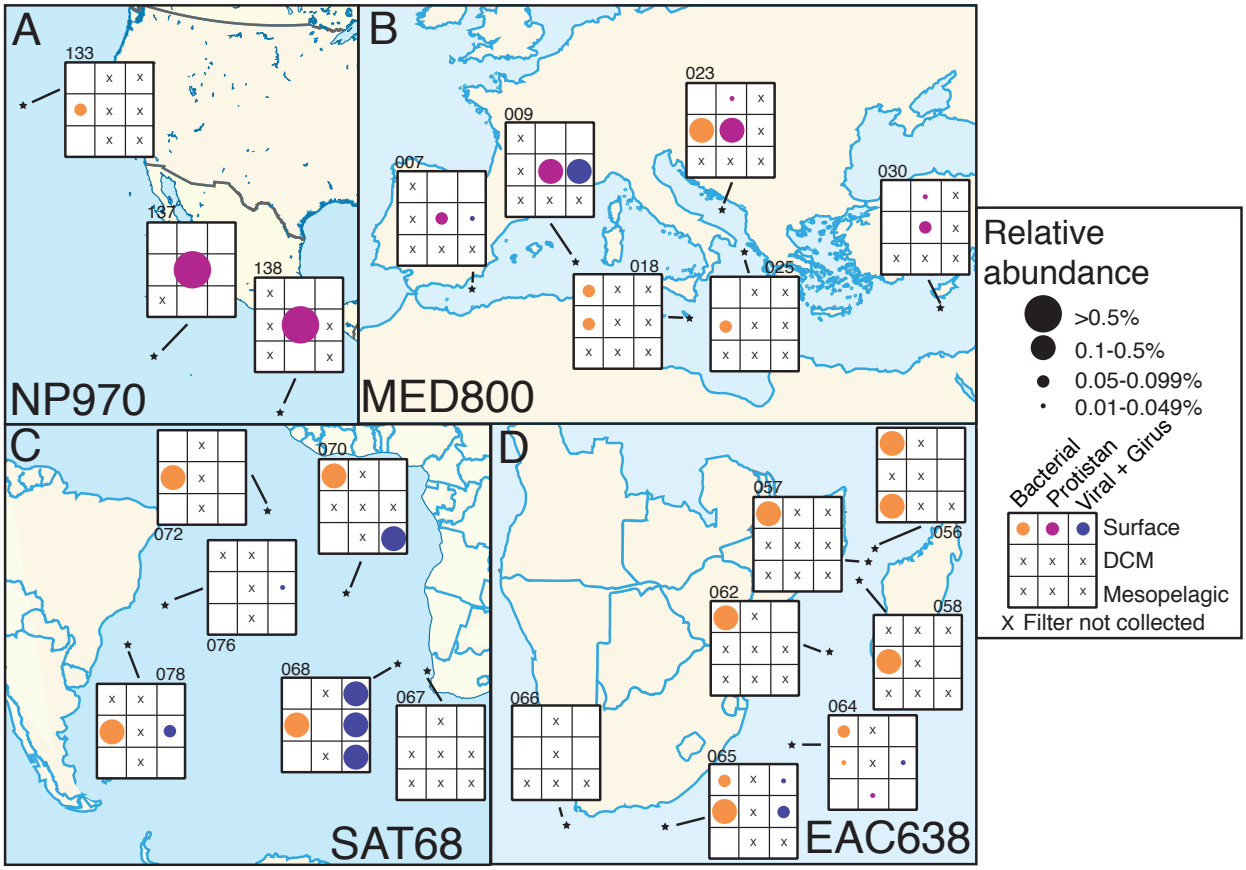

Fig. 1. The approximate locations of *Tara Oceans* sampling sites used to generate metagenomes incorporated in to this study. Each grid represents the three possible sample depths and filter fractions (top row: surface, middle row: DCM, bottom row: mesopelagic). An 'X' denotes that no sample was collected for that depth and size fraction at the site. Circle size represents relative abundance. (A) North Pacific – NP 970, (B) Mediterranean Sea – MED800, (C) South Atlantic – SAT68, and (D) East Africa current – EAC638. Size fraction: orange, 'bacterial' (0.22-1.6µm); purple, 'protistan' (0.8-5.0µm); blue, 'girus'+'viral' (<0.22-0.8µm).

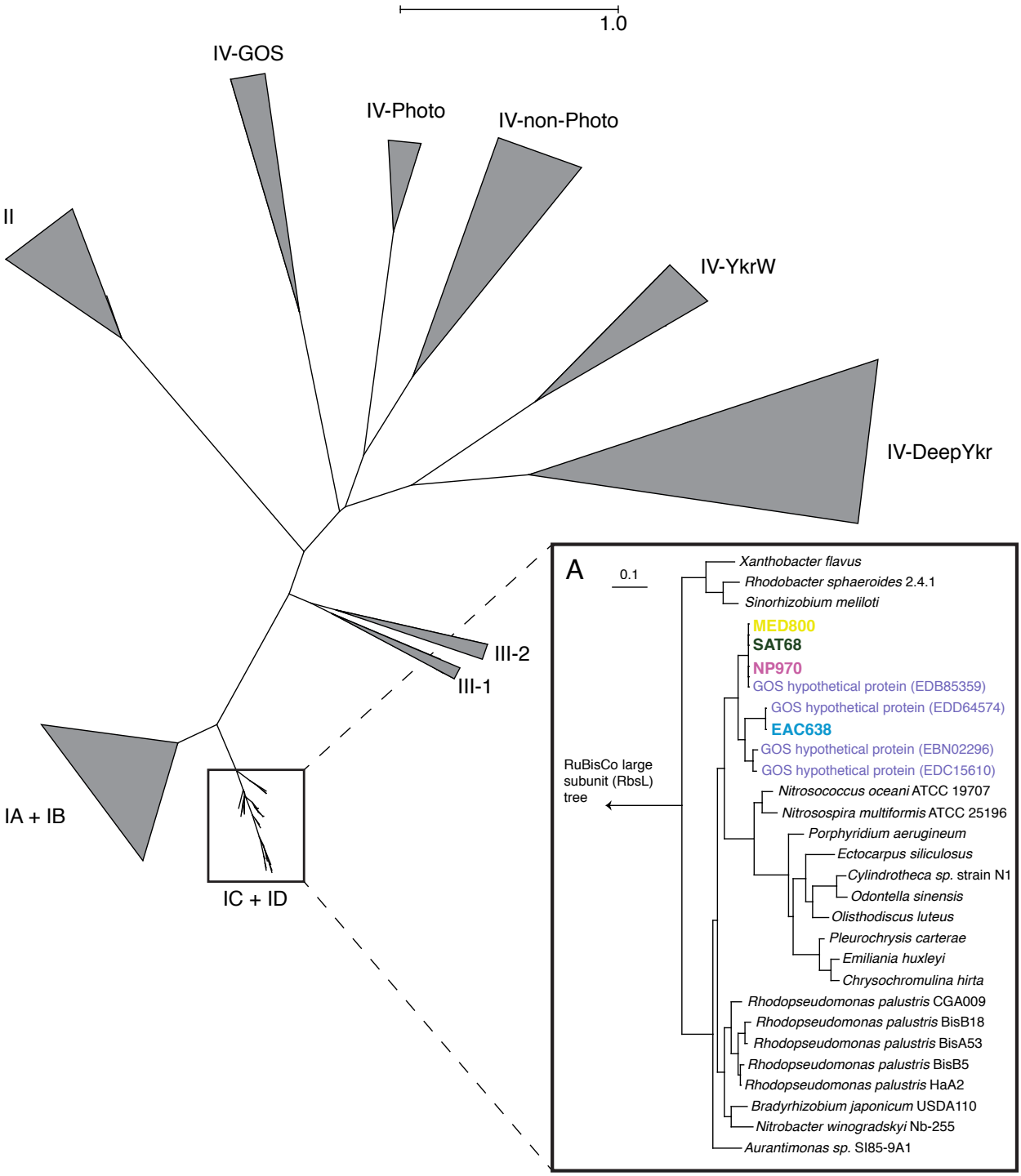

Fig. 2. Phylogenetic tree of the ribulose-1,5-bisphosphate carboxylase large subunit (Rubsico, RbsL) with the major forms denoted. Inset (**A**) – A zoomed in view of the Type 1C/D Rubsico subgroup. Purple sequence names denote RbsL proteins from the Global Ocean Survey. Sequences used for this tree can be found in Supplementary Information 10. Phylogenetic distances and local support values can be found in Supplementary Information 12. Sequence information, including accession numbers and assignments can be found in Supplementary Information 8.

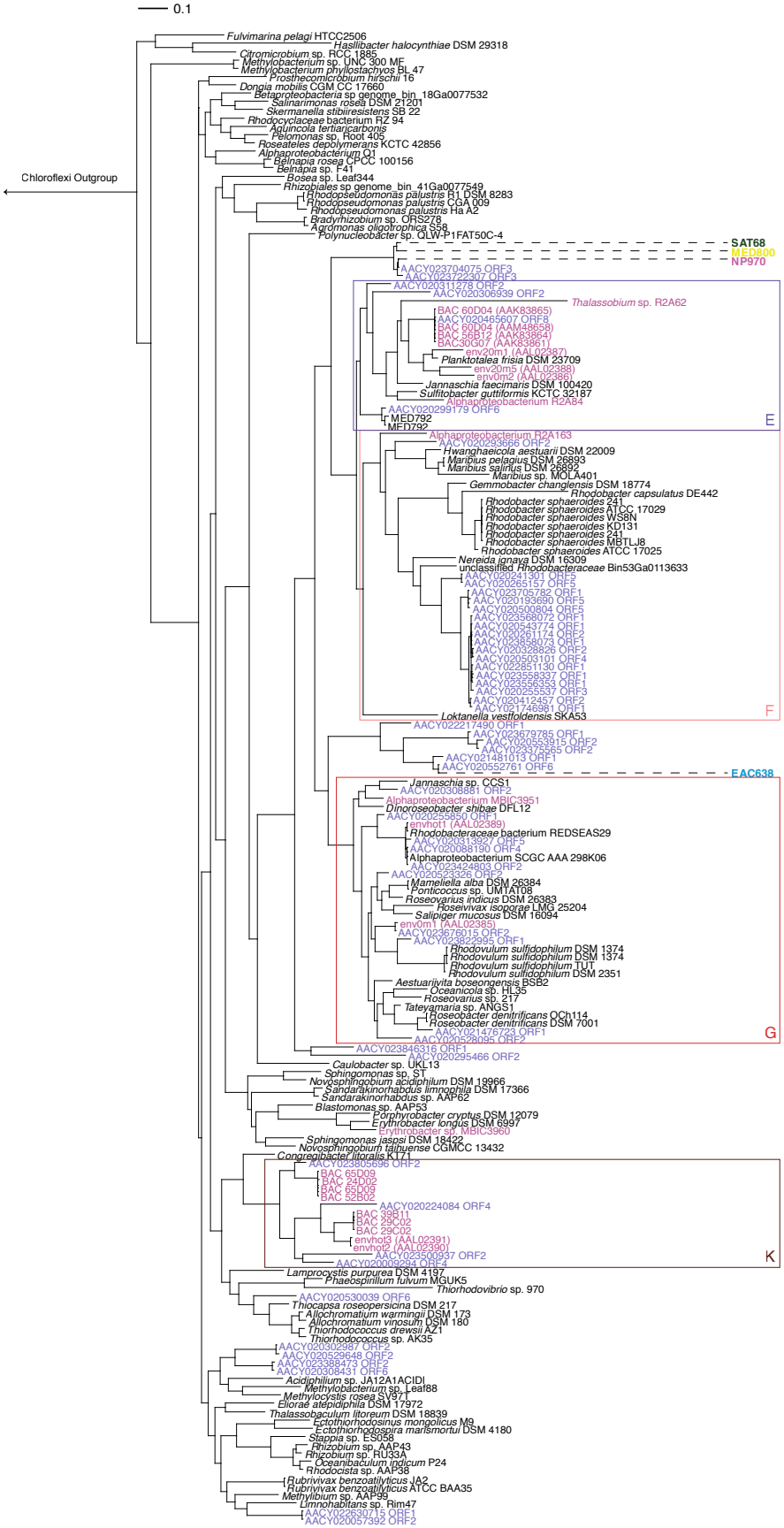

396 **Extended Data Fig. 3**. Phylogenetic tree of the M subunit of type-II photochemical reaction
397 center (PufM). Environmental sequences obtained from the Global Ocean Survey (purple, •) and
398 *Béjá et al.* (2002) (pink, •) are highlighted. Boxes illustrate approximate positions of
399 phylogroups previously assigned by Yutin *et al.* (2007). Sequences used for this tree can be
400 found in Supplementary Information 11. Phylogenetic distances and local support values can be
401 found in Supplementary Information 13. Sequence information, including accession numbers and
402 taxonomies can be found in Supplementary Information 9.
403

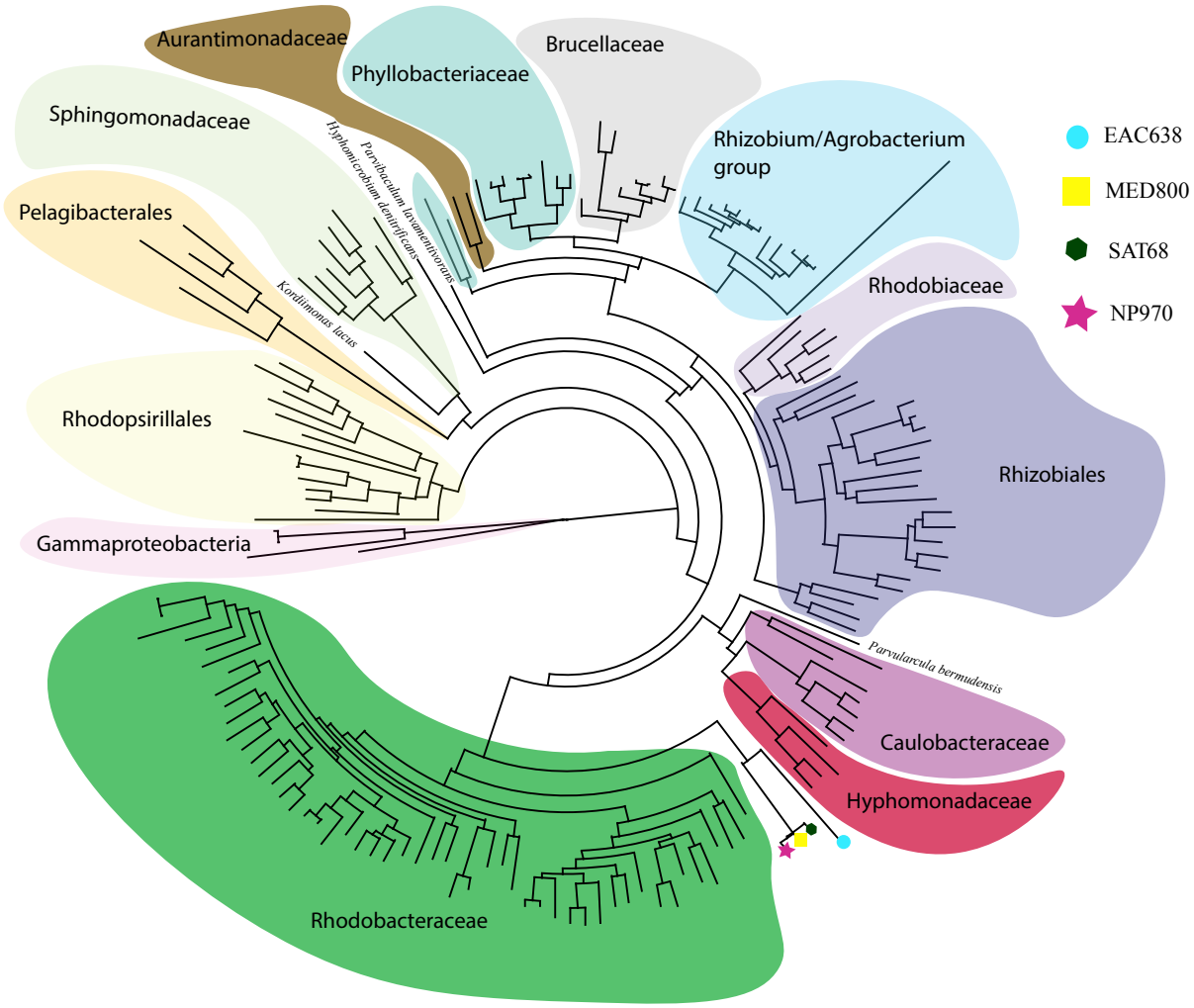

404

405 **Fig. 4**. Approximate maximum likelihood *Alphaproteobacteria* phylogenetic tree of 17
406 concatenated single-copy marker genes for the *Tara* assembled and 160 reference genomes.
407 Reference sequences from the *Gammaproteobacteria* used as an outgroup. Reference genome
408 information, including accession numbers, can be found in Supplementary Information 4.
409 Phylogenetic distances and local support values can be found in Supplementary Information 5.
410

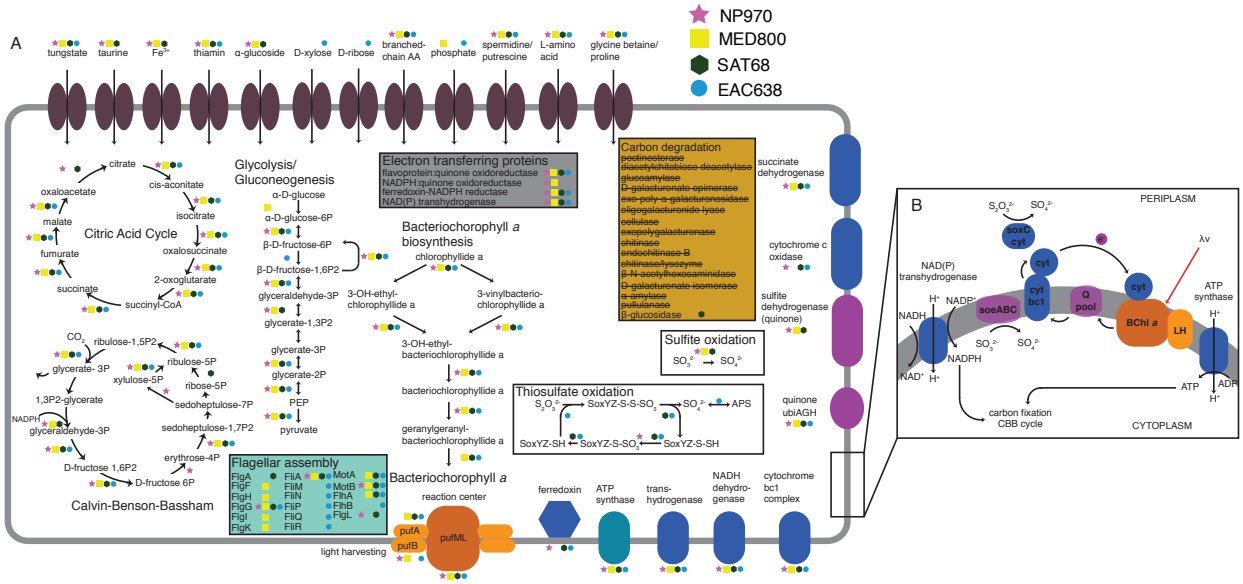

411

412 **Fig. 5**. Cellular schematic of the four reconstructed genomes. (**A**) The presence of a gene(s) in a
413 genome is represented by a yellow square (MED800), pink star (NP970), green hexagon
414 (SAT68), and/or blue circle (EAC638). Schematic illustrates predicted membrane bound
415 proteins, but does accurately represent cellular localization. (**B**) A detailed view of the proposed
416 flow of electrons from donors to photosynthesis and carbon fixation. Abbreviations: cyt,
417 cytochrome; Q pool, quinone pool; BChl *a*, bacteriochlorophyll a; LH, light-harvesting proteins;
418 soeABC, sulfite dehydrogenase (quinone); CBB, Calvin-Benson-Bassham.
419

420 **Table 1**. Statistics of the four *Tara* assembled genomes.

Genome ID	No. of contigs	Total length (bp)	Max. contig length (bp)	N50	Mean length (bp)	GC (%)	No. of predicted CDS◊	Est. Completeness (%)*	Est. duplication/redundancy (Est. strain heterogeneity) (%)*
MED800	**174**	**2,140,579**	**55,951**	**13,831**	**12,302**	**36.7**	**2,184**	**66.98**	**2.36 (100.0)**
SAT68	**192**	**2,295,506**	**63,422**	**13,440**	**11,956**	**36.8**	**2,334**	**85.02**	**5.37 (75.0)**
EAC638	**121**	**1,868,409**	**80,916**	**19,502**	**15,441**	**30.7**	**1,939**	**68.88**	**4.75 (75.0)**
NP970	**120**	**2,585,639**	**84,649**	**32,137**	**21,547**	**36.1**	**2,445**	**82.04**	**3.04 (33.33)**

421 ◊, as determined using Prodigal
422 *, as determine using CheckM with the Alphaproteobacteria markers (225 markers in 148 sets)
423 N50 - length of contig for which all contigs longer in length contain half of the total genome
424 CDS - coding DNA sequence
425

426 **Supplementary Materials:**

427 Extended Data Figures 1-6

428 Extended Data Table 1

429 Supplementary Information 1-13

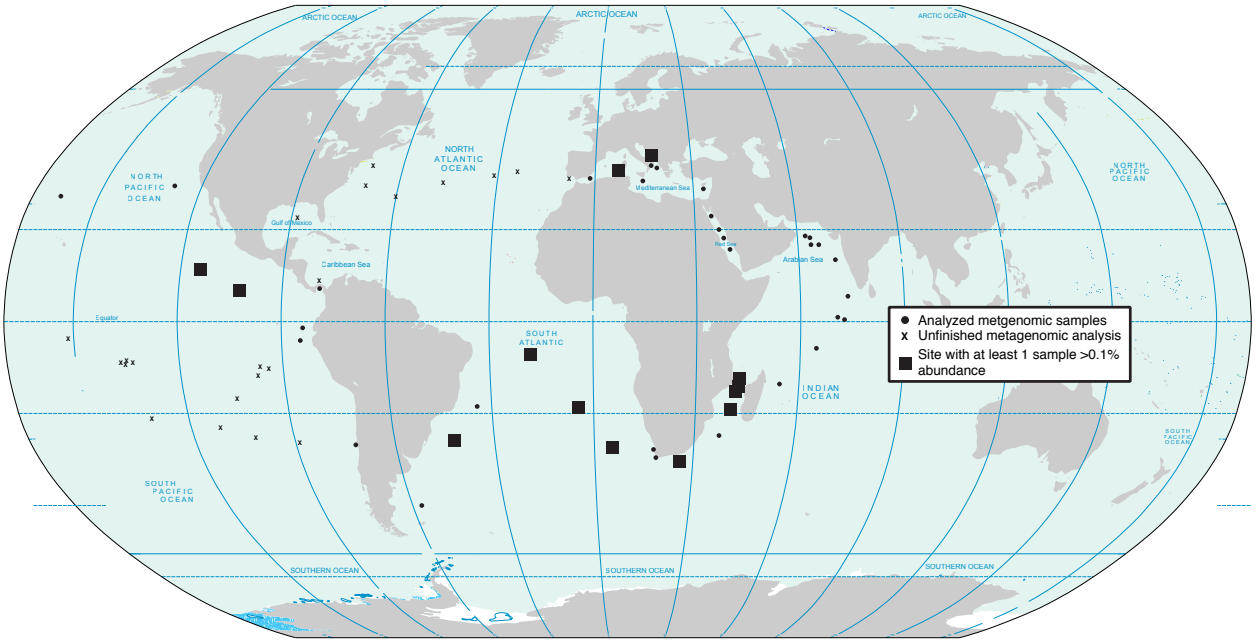

430

431 **Extended Data Fig. 1**. A map illustrating the approximate locations of the *Tara Oceans*
432 sampling stations. Stations and samples with >0.1% relative abundance of the *Tara* assembled
433 genomes are emphasized. Circles - stations for which metagenomes have been assembled,
434 genomes have been reconstructed, and cursory functional analysis has been performed. Exes –
435 stations awaiting assembly, binning, and analysis. Squares – stations where at least 1 sample had
436 >0.1% abundance of the *Tara* assembled genomes.

437

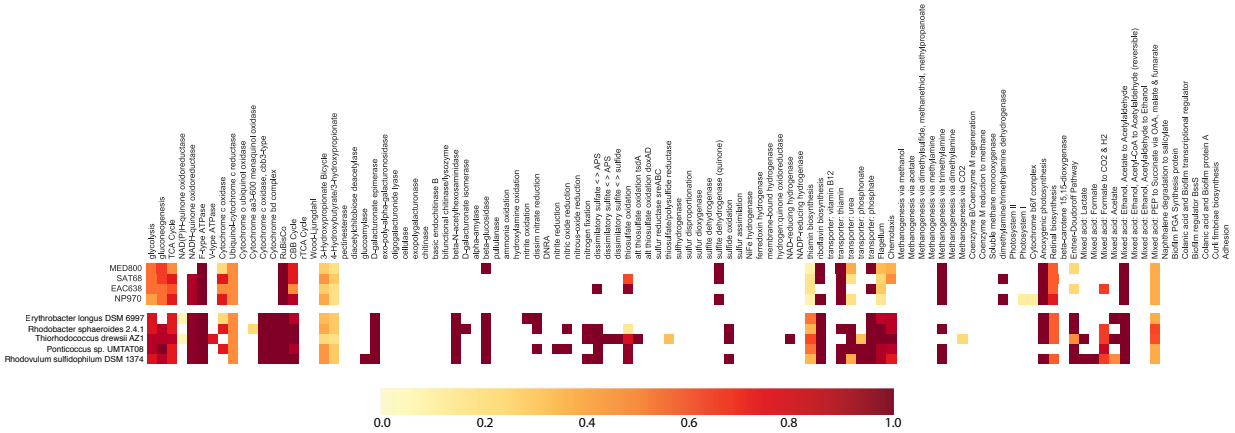

438

439 **Extended Data Fig. 2**. A heat map demonstrating the degree of completeness of various
440 pathways and genes determined for the four *Tara* assembled genomes. Additionally, the same
441 process was applied to genomes of confirmed anaerobic anoxygenic photoautotrophs for
442 comparison. Pathways are linked to KEGG Ontology identifiers and the figure was generated
443 using the script KEGG-decoder.py.

444

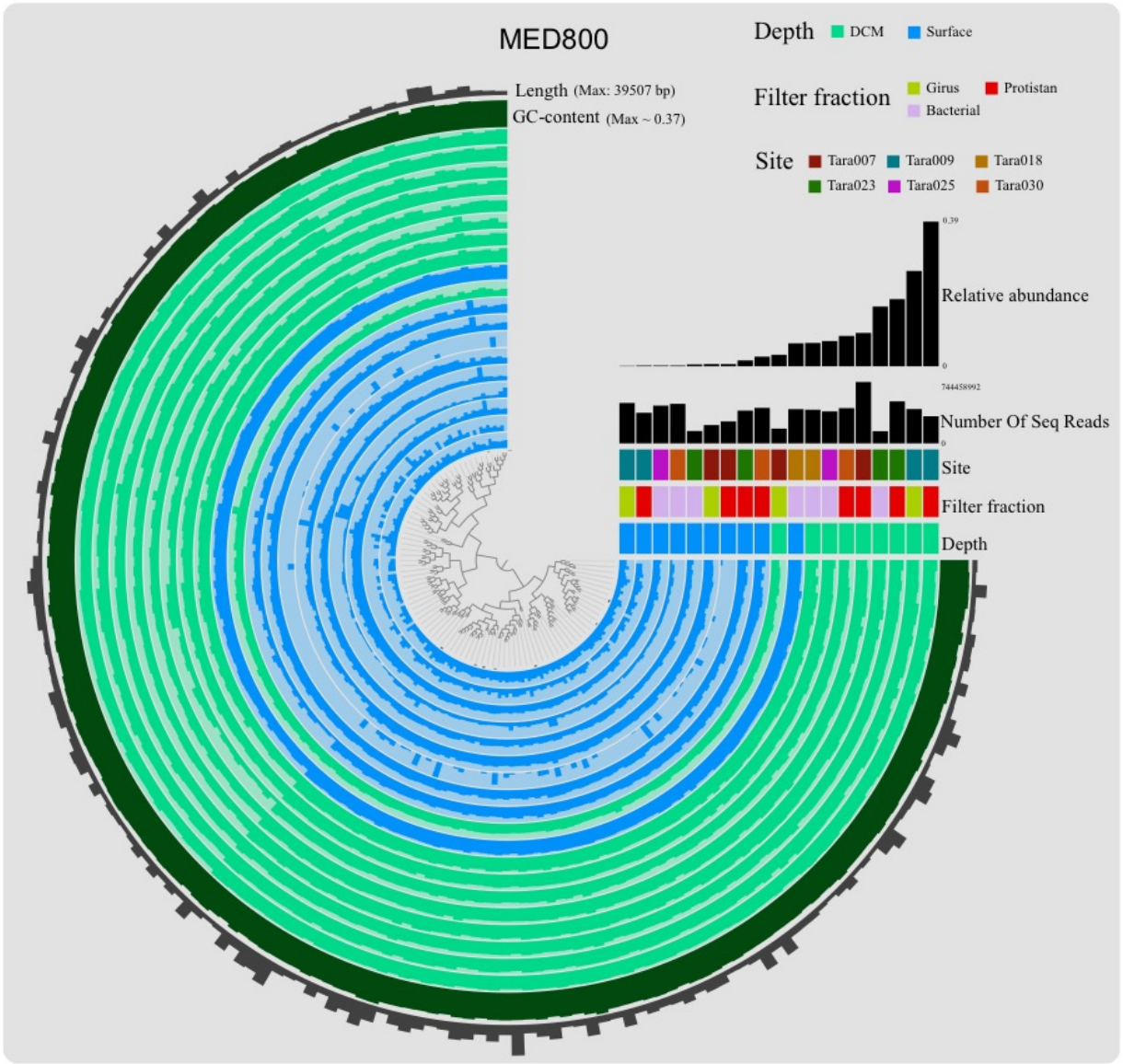

Extended Data Fig. 3. Visualization of MED800 using Anvi'o. Contigs are clustered in Anvi'o using Ward distance hierarchical clustering combining sequence composition and coverage information. Standardized coverage is shown for each sample. Relative abundance, number of sequencing reads generated, site, filter fraction, and depth are all shown. Completion, contamination, and strain heterogeneity were produced using CheckM.

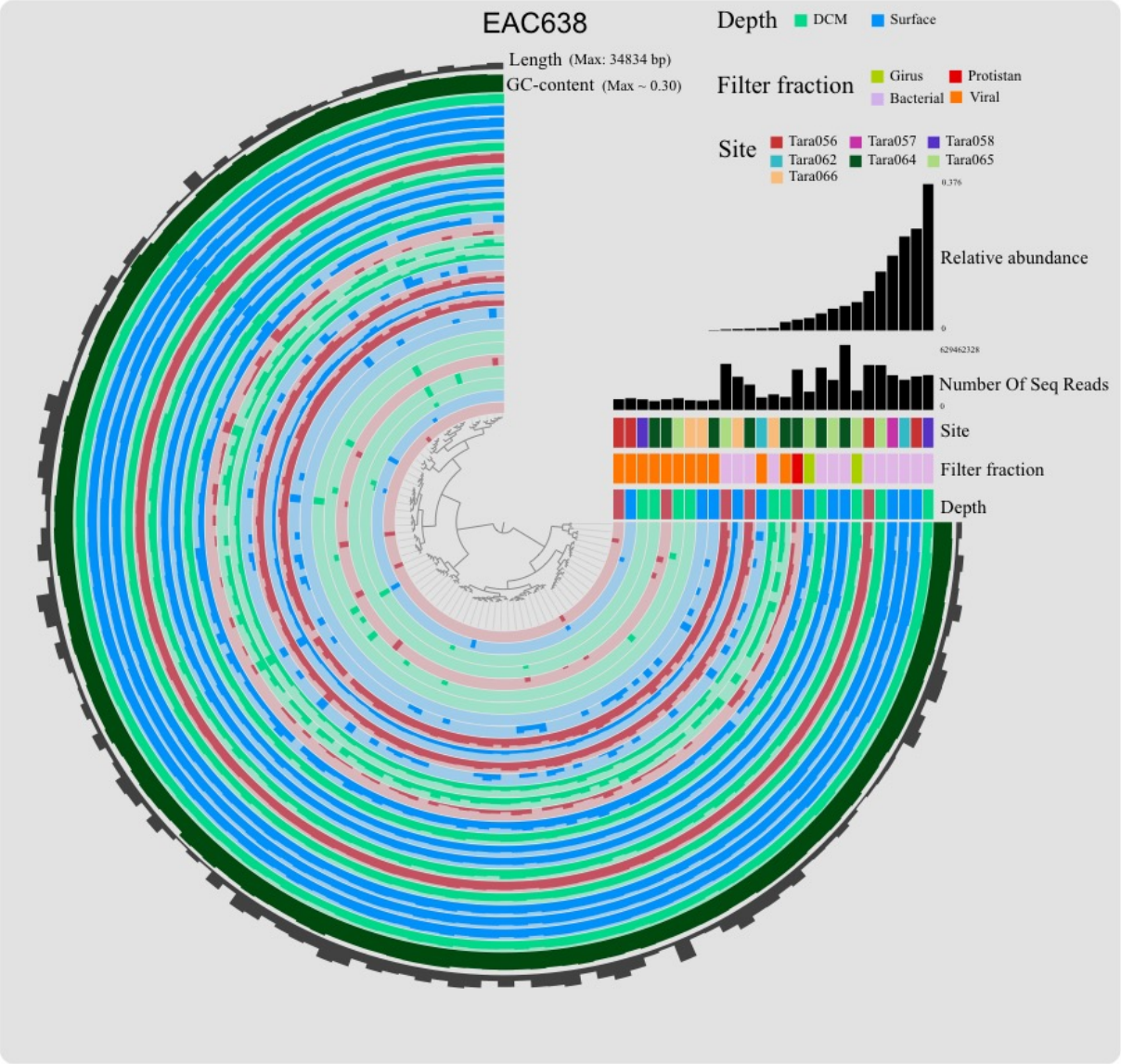

Extended Data Fig. 4. Visualization of EAC638 using Anvi'o. Contigs are clustered in Anvi'o using Ward distance hierarchical clustering combining sequence composition and coverage information. Standardized coverage is shown for each sample. Relative abundance, number of sequencing reads generated, site, filter fraction, and depth are all shown. Completion, contamination, and strain heterogeneity were produced using CheckM.

460

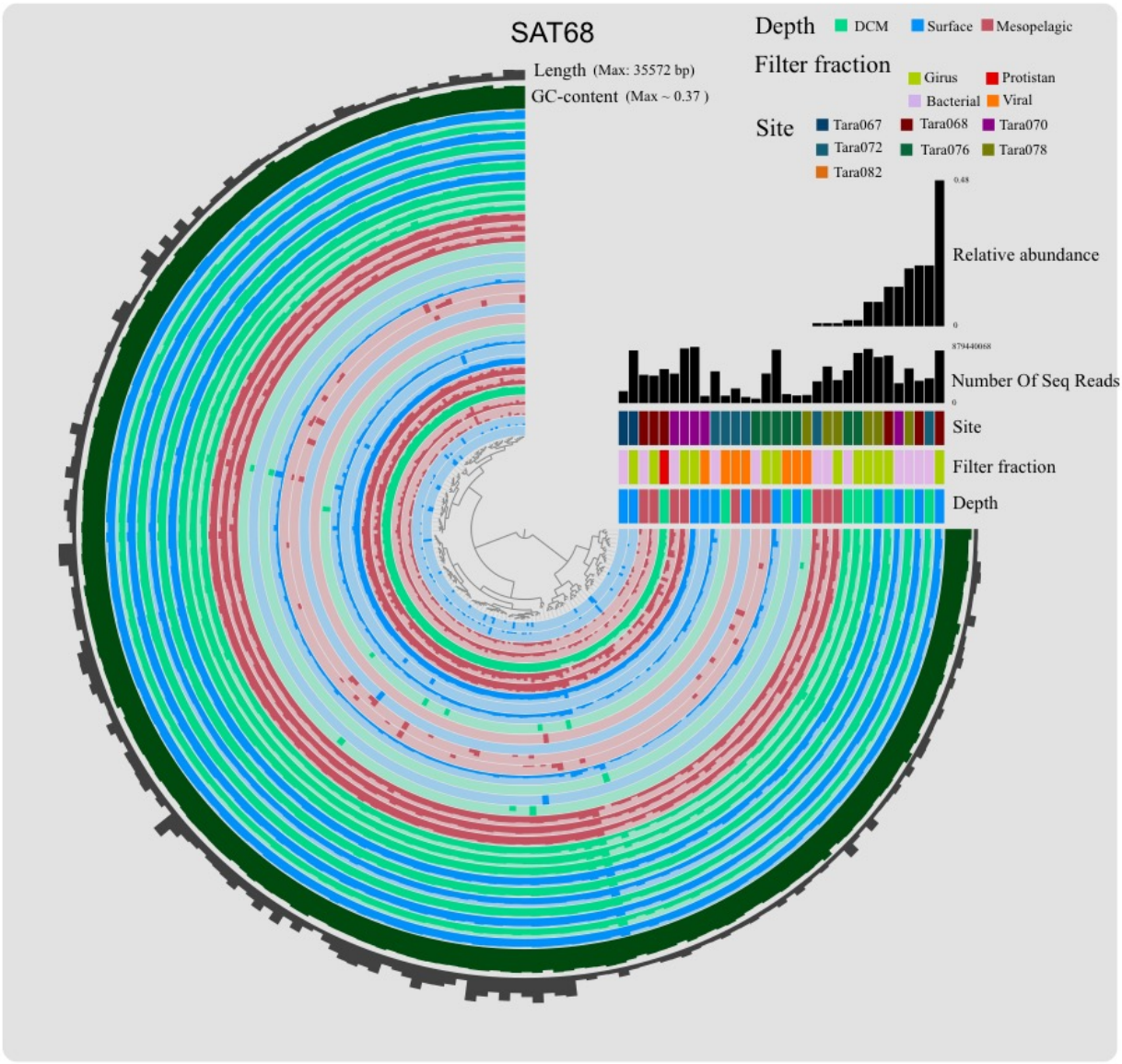

461

462 **Extended Data Fig. 5**. Visualization of SAT68 using Anvi'o. Contigs are clustered in Anvi'o
463 using Ward distance hierarchical clustering combining sequence composition and coverage
464 information. Standardized coverage is shown for each sample. Relative abundance, number of
465 sequencing reads generated, site, filter fraction, and depth are all shown. Completion,
466 contamination, and strain heterogeneity were produced using CheckM.

467

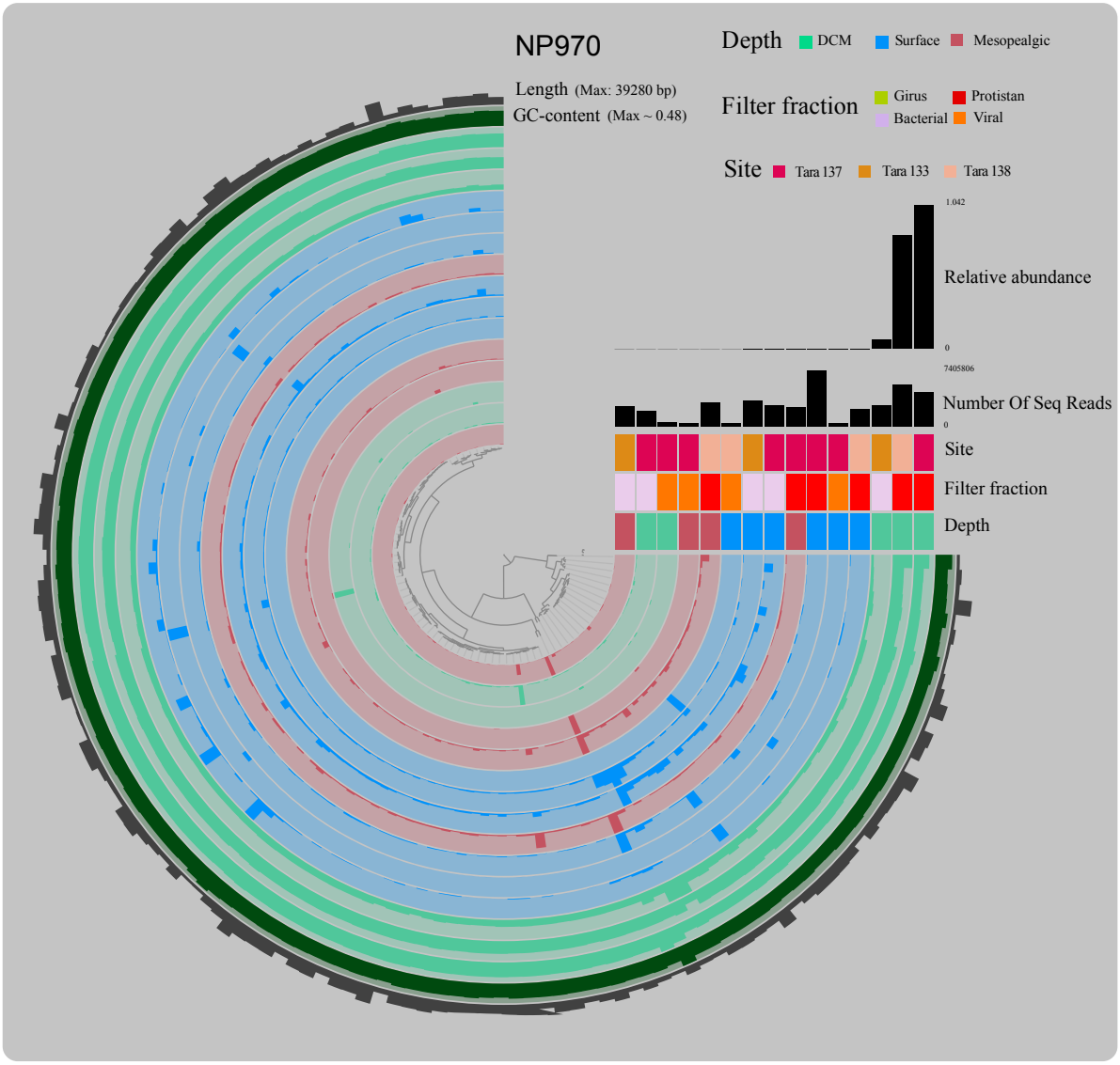

Extended Data Fig. 6. Visualization of NP970 using Anvi'o. Contigs are clustered in Anvi'o using Ward distance hierarchical clustering combining sequence composition and coverage information. Standardized coverage is shown for each sample. Relative abundance, number of sequencing reads generated, site, filter fraction, and depth are all shown. Completion, contamination, and strain heterogeneity were produced using CheckM.

475

476 **Extended Data Table 1**. Single-copy marker genes identified in each of the putative AAnP and
477 reference genomes with corresponding Pfam identifiers.

478

Marker Gene Names	
Aminoacyl tRNA synthetase class II, N-terminal domain	PF02912
GTP1/OBG	PF01018
RecA	PF00154
Ribosomal L17	PF01196
Ribosomal L25p family	PF01386
Ribosomal L28 protein	PF00830
Ribosomal protein L20	PF00453
Ribosomal protein L31	PF01197
Ribosomal protein L35	PF01632
Ribosomal protein L6	PF00347
Ribosomal protein S11	PF00411
Ribosomal protein S13/S18	PF00416
Ribosomal protein S14	PF00253
Ribosomal protein S15	PF00312
Ribosomal protein S4/S9 N-terminal domain	PF00163
Ribosomal protein S5, N-terminal domain	PF00333
RNA polymerase Rpb3/Rpb11 dimerisation domain	PF01193

479

Supplementary Information 1. Information and statistics of the Tara stations and samples from the North Pacific, Mediterranean Sea, East Africa Coastal province, and South Atlantic. Includes, station, size fraction, depth, number of paired-end reads assembled, number of assemblies generated by Megahit, and relative abundance values for each genome.

Supplementary Information 2. Information about genes specifically referenced in manuscript and figures. Includes, KO identifiers, gene names, and gene abbreviations.

Supplementary Information 3. BlastKOALA annotations of the Prodigal predicted genes for each of the four genomes.

Supplementary Information 4. List of 2,889 reference genomes used to construct the *Alphaproteobacteria* phylogenetic tree.

Supplementary Information 5. Newick format of the *Alphaproteobacteria* phylogenetic tree containing 2,889 reference genomes. Contains branch lengths and local support values.

Supplementary Information 6. List of 85 reference genomes used to construct the *Alphaproteobacteria* phylogenetic tree in Figure 2.

Supplementary Information 7. Newick format of the *Alphaproteobacteria* phylogenetic tree containing X reference genomes. Contains branch lengths and local support values.

Supplementary Information 8. List of reference sequences used to construct the ribulose-1,5-bisphosphate carboxylase large subunit phylogenetic tree. Sequences collected from Tabita *et. al.* (2007).

Supplementary Information 9. List of reference sequences used to construct the photosynthetic reaction center M subunit phylogenetic tree. Sequences collected from Yutin *et. al.* (2007).

Supplementary Information 10. Sequences used to construct the ribulose-1,5-bisphosphate carboxylase large subunit phylogenetic tree in FASTA format.

Supplementary Information 11. Sequences used to construct the photosynthetic reaction center M subunit phylogenetic tree in FASTA format.

Supplementary Information 12. Newick format of the ribulose-1,5-bisphosphate carboxylase large subunit phylogenetic tree. Contains branch lengths and local support values.

Supplementary Information 13. Newick format of the photosynthetic reaction center M subunit phylogenetic tree. Contains branch lengths and local support values.